PROCEEDINGS OF SPIE

SPIEDigitalLibrary.org/conference-proceedings-of-spie

Knotted topologies in the polarization state of bichromatic light

Emilio Pisanty

Emilio Pisanty, "Knotted topologies in the polarization state of bichromatic light," Proc. SPIE 11818, Laser Beam Shaping XXI, 1181809 (1 August 2021); doi: 10.1117/12.2596834

SPIE.

Event: SPIE Optical Engineering + Applications, 2021, San Diego, California, United States

Invited Paper

Knotted topologies in the polarization state of bichromatic light

Emilio Pisanty[a,b]

[a]ICFO—Institut de Ciencies Fotoniques, The Barcelona Institute of Science and Technology, 08860 Castelldefels, Barcelona, Spain
[b]Max Born Institute for Nonlinear Optics and Short Pulse Spectroscopy, Max Born Strasse 2a, D-12489 Berlin, Germany

ABSTRACT

The fundamental polarization singularities of light are generally symmetric under coordinated rotations: that is, transformations which rotate the spatial dependence of the fields by an angle θ and the field polarization by a fraction $\gamma\theta$ of that angle, as generated by 'mixed' angular momenta of the form $L + \gamma S$. Generically, the coordination parameter γ has been thought to be restricted to integer or half-integer values. In this work we show that this constraint is an artifact of the restriction to monochromatic fields, and that a wider variety of optical singularities is available when more than one frequency is involved. We show that these new optical singularities present novel field topologies, isomorphic to torus knots, and we show how they can be characterized both analytically and experimentally. Moreover, the generator for the symmetry group of these singularities, whose algebraic structure is deeply related to the torus-knot topology of the beams, is conserved in nonlinear optical interactions.

Keywords: Topological optics, singular optics, structured light, optical singularities, polarization singularities, rotational invariance, nonlinear optics, high-harmonic generation

This work reviews, summarizes and contextualizes the results previously reported in Refs. 1, 2.

1. INTRODUCTION

The rotational invariance of optics is one of the central features of the theory, and it is central to the conservation of angular momentum, both within electromagnetism in general as well as within optics in particular. As such, rotationally-invariant beams are one of the central conceptual pillars that underpin our understanding of optics. The simplest example of this are beams with circular polarization (depicted in Fig. 1(a)), which are invariant under rotations of the electric- and magnetic-field polarization of the beam: if an optical beam polarized as $\mathbf{E} = E_0\hat{\mathbf{e}}_\pm$ (where $\hat{\mathbf{e}}_\pm = (\hat{\mathbf{e}}_x \pm i\hat{\mathbf{e}}_y)/\sqrt{2}$) is rotated by an angle α, it acquires a phase, $R(\alpha)\mathbf{E} = e^{\pm i\alpha}\mathbf{E}$, equivalent to a time delay.

A more recent discovery is that of light beams that are invariant under rotations to their spatial dependence, the most prominent of which are Laguerre-Gauss (LG) beams (whose relationship with the orbital angular momentum (OAM) of light[3] launched the field of structured light[4–7]). These beams have helical wavefronts as show in Fig. 1(b), so if the spatial dependence is rotated, the beam again acquires a phase: $E(R(\alpha)^{-1}\mathbf{r})) = e^{im\alpha}E(\mathbf{r})$, where m is the OAM quantum number of the beam. Moreover, this rotational invariance (associated with a well-defined OAM L_z along the optical axis) can be combined with polarization rotational invariance (associated by the spin angular momentum (SAM) S_z) to give beams that are invariant under full physical rotations of the beam (i.e. combined rotations of the polarization and the spatial dependence, generated by the total optical angular momentum J_z). This includes beams with radial and azimuthal polarizations (shown in Fig. 1(c,d)) as well as similar optical polarization singularities.

However, while they are enormously useful, the polarization singularities of vector beams invariant under full physical rotations are not the most fundamental or the most stable optical singularities, and if they are, e.g.,

emilio.pisanty@mbi-berlin.de

Laser Beam Shaping XXI, edited by Angela Dudley, Alexander V. Laskin,
Proc. of SPIE Vol. 11818, 1181809 · © 2021 SPIE · CCC code:
0277-786X/21/$21 · doi: 10.1117/12.2596834

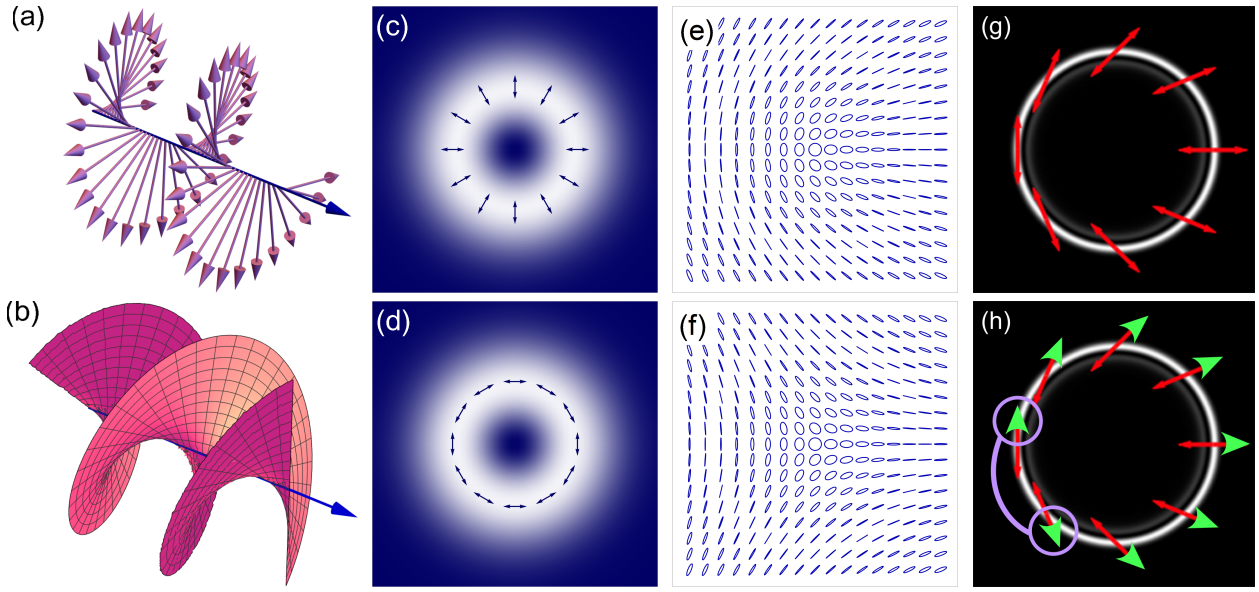

Figure 1. Rotationally-invariant beams. (a) Circularly-polarized beam, invariant under rotations of polarization. (b) Optical vortex with a helical wavefront, invariant under rotations of the spatial dependence of the field. (c,d) Radially- and azimuthally-polarized beams, invariant under full physical rotations. (e,f) 'Lemon' and 'star' C-points, invariant under coordinated rotations. (g) Similar field with locally-linear polarization, produced by conical refraction (adapted under CC BY-NC from Ref. 8). (h) Nontrivial Möbius-band topology of the polarization field in (g).

propagated through a turbulent medium, the singularity is liable to break up into individual singularities of a more fundamental nature. These singularities are known as C-points, and two examples are shown in Fig. 1(e,f): these are points where the field is circularly polarized, surrounded by points of elliptical polarization; moreover, if one moves in a circle around the singularity, the direction of this elliptical polarization performs a full 180° rotation. This can be either with the direction of traversal – in which case the C-point is of 'lemon' type, as in Fig. 1(e) – or against it, as in Fig. 1(f),in which case it is known as a 'star' point.

At an initial look, the polarization fields of the C-point optical singularities in Fig. 1(e,f) look anisotropic and asymetric, but they do have a rigid symmetry: they are invariant under *coordinated rotations*,

$$\mathbf{E}(\mathbf{r}) \mapsto R(\gamma\alpha)\mathbf{E}(R(\alpha)^{-1}\mathbf{r}), \tag{1}$$

in which the spatial dependence is rotated by an angle α but its polarization is rotated by an angle $\gamma\alpha$, which is related to the spatial-dependence rotation angle α by the *coordination parameter* γ. For the 'lemon' and 'star' C-points of Fig. 1(e,f), γ equals $+1/2$ and $-1/2$, respectively. Moreover, this analysis can be made simpler if we restrict our attention to beams whose polarization is always (locally) linear, which can be achieved using conical refraction[8–10] as shown in Fig. 1(g), with the only requirement that the optical singularity should now be dark.

Once we adopt this frame, however, a strong contradiction emerges. In general, our descriptions for linearly-polarized light involve a real-valued polarization vector $\mathbf{E}(\mathbf{r})$, which can vary over space, and this corresponds to adding an arrowhead to each of the polarization directions in Fig. 1(g) to select a direction. This can indeed be done locally, but, as we show in Fig. 1(h), if we attempt to do this globally over the entire beam, we are doomed to failure: since the polarization rotates by 180° over a 360° traversal around the beam, when we return to our original starting point the arrowhead has flipped its orientation.

Physically, the resolution of this apparent contradiction is that, as we traverse the beam, the field acquires a growing phase which reaches a full sign-flip phase of $e^{i\pi} = -1$ when we return to the starting point, accounting for the flipped direction. Topologically, however, things are much more interesting, because the mismatched orientations in Fig. 1(h) tell us that the beam has the topology of a Möbius band. (Indeed, this topology can be explicitly achieved in three dimensions by using nonparaxial configurations, as has been shown both theoretically[11,12] and experimentally.[13–15]) This Möbius-band topology is only possible if the coordination

parameter γ is either an integer or a half-integer, a restriction which is further reinforced by the fact that the only internal symmetry of monochromatic light is a rotation by 180° associated with a half-period delay.

Because of this, it has long been assumed (and recently 'proved' with rigorous arguments[8]) that the only possible values for the coordination parameters that yield nontrivial beams invariant under the coordinated-rotation symmetry of (1) are integers and half-integers. However, as we shall explain below, following our previous results fromRef. 1, this restriction is an artefact produced by restricting our theoretical framework to monochromatic light. If this artificial restriction is broken, and polychromatic beams are allowed, the full spectrum of coordination parameters γ becomes available, bringing with it a wide array of novel possible topologies for the electromagnetic field.

2. TORUS-KNOT BEAMS

The key pillar that allows this conceptual expanse is that of the 'bicircular' polarization of light: that is, the coherent superposition of two counter-rotating circularly-polarized light fields at different frequencies, with the archetypal combination being a fundamental ω and its second harmonic 2ω, which has been an essential

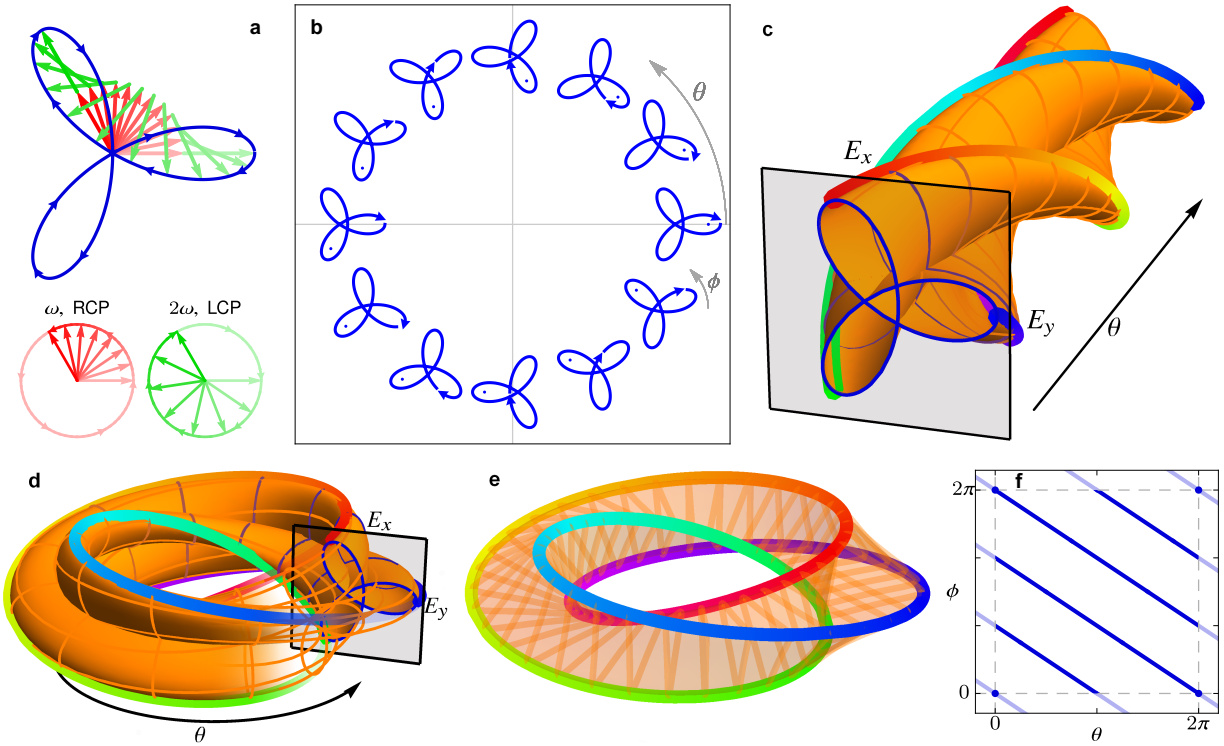

Figure 2. Coordinated-rotation invariance and torus-knot beam topology. (a) The superposition of a right-circularly polarized beam (red) with its left-circularly polarized second harmonic (green) produces a trefoil-shaped polarization Lissajous figure (blue). The orientation of this trefoil depends on the relative phase between the two components, which can be made to vary along the azimuthal position θ by adding different orbital angular momenta m_1 and m_2 to the two components, shown in (b) for $m_1 = 0$ and $m_2 = -2$: the field then has coordinated-rotation invariance of the form $R(\gamma\alpha)\mathbf{E}(\theta - \alpha, t) = \mathbf{E}(\theta, t + \tau\alpha)$ with coordination parameter $\gamma = -2/3$ and $\tau = 1/6\omega$, and the lobe marked with a dot does not return to itself after a 2π azimuthal traversal over θ. (c) To study this field's topology, we unfold the polarization and azimuthal dependence, and then (d) twist the resulting cylinder to reconnect the planes at $\theta = 0$ and 2π. (e) If we then retain only the paths of the tips of the trefoil lobes (coloured by hue on (c-e) for visual clarity only), we obtain a knotted curve embedded on a torus, in this case the $(-2, 3)$ torus knot. (f) This torus knot can be seen as the path of the lobes on the flat torus $[0, 2\pi) \times [0, 2\pi)$ of the azimuthal and polarization angles θ and ϕ, but also as the coordinated rotations when seen as a subgroup of the independent-rotations group $\mathrm{SO}(2) \times \mathrm{SO}(2)$. 3D-printable models of (d) and (e) are available from Ref. 16. Figure reproduced from Ref. 1.

tool in the study of high-harmonic generation (HHG) as it offers a simple way to generate circularly-polarized harmonics.[17,18] This combination, shown in Fig. 2(a), produces a trefoil-shaped Lissajous figure for the electric field, which has a *three*-fold internal symmetry: a time delay by 1/3 of the period of the fundamental is equivalent to a 120° rotation of the polarization.

This new internal symmetry of the local polarization state of the light then allows us to break the monochromatic restriction to half-integer coordination parameters. To do this, as shown in Fig. 2(b), we simply shape the two frequency components into Laguerre-Gauss modes with different OAM quantum numbers, which gives them a different relative phase at different azimuthal positions along the beam. Since the relative phase between the two components governs the orientation of the resulting trefoil, the combination produces a field of trefoil polarizations which are rotated with respect to each other.

The crucial new feature becomes apparent if we label one of the trefoil lobes in Fig. 2(b) with a dot, and then follow this individual lobe along the azimuthal traverse around the beam in the figure as the trefoil turns: when we return to our starting point, the trefoil returns to the same global shape, but the dot marking the lobe we are following has switched to a neighbour. This is precisely the same topological nontriviality we observed in Fig. 1(h) for C-point and conical-refraction beams, except that the usual two-stranded Möbius-strip topology now has *three* strands we must follow, thus giving a novel topology.

To understand this topology, we first fold out the azimuthal component of the position, θ, as a separate ("synthetic"[19]) dimension, orthogonal to the electric-field plane occupied by the bicircular trefoil, as pictured in Fig. 2(c). Here we see the lobes of the trefoil twist around in a helix as θ goes from 0 to 2π, and there the electric-field plane at the back of the figure is a copy of the plane at the front at $\theta = 0$, so we can twist the figure around, as in Fig. 2, to join the two. Distilling away most of the complexity of the figure to retain only the positions of the lope tips represented by the multicolored line, we get a simple expression of the topology, shown in Fig. 2(e).

The novel topology is now fully revealed: the lobe-tip curve is knotted into itself, and cannot be smoothly deformed back into a single loop without intersecting itself. More technically, it forms a *torus knot*, since the curve can be naturally embedded in a torus, and as such it can be classified using a pair of indices, (n, m), which count the number of crossings of the two independent 'equators' of the torus. For the specific case of Fig. 2, these indices are $(-2, 3)$, and they are in direct correspondence with the correlation parameter $\gamma = -2/3$ of the beam. This is a general feature: the indices of torus knots are isomorphic to a fraction, and this fraction is in strict correspondence with the coordination parameter of the beam for any bichromatic combination with commesurate frequencies $p\omega$ and $q\omega$, which is given by

$$\gamma = \frac{m_2\omega_1 - m_1\omega_2}{\omega_1 + \omega_2} = \frac{m_2 p - m_1 q}{p + q}, \tag{2}$$

where m_1 and m_2 are the OAM quantum numbers of the first and second beams, respectively.

3. THE SYMMETRY GENERATOR

In most cases, when one looks for optical fields which are invariant under a symmetry transformation, the goal is to find a symmetry generator $\hat{\mathcal{G}}$ and a complex-amplitude vector field $\tilde{\mathbf{E}}(\mathbf{r})$ which is an eigenfunction of the generator,

$$\hat{\mathcal{G}}\,\tilde{\mathbf{E}}(\mathbf{r}) = g\tilde{\mathbf{E}}(\mathbf{r}), \tag{3}$$

and therefore also of the symmetry itelf, since it follows that

$$e^{i\hat{\mathcal{G}}}\,\tilde{\mathbf{E}}(\mathbf{r}) = e^{ig}\,\tilde{\mathbf{E}}(\mathbf{r}), \tag{4}$$

for a complex phase e^{ig}; in general, this framework is completely sufficient for all applications to monochromatic light. In our case, however, the beam is not monochromatic, which adds a substantial complication in that the complex phase e^{ig} no longer has a clear meaning, as it does not have a single clear-cut relationship with time. (Indeed, for the two different components at frequencies ω_1 and ω_2, complex phase accumulates at different

rates: $e^{-i\omega_1 t}$ and $e^{-i\omega_2 t}$, respectively.) Because of this, we must discard the abstracted eigenfunction-eigenvalue relation of (3) and return to its roots.

At its core, expression (4) describes a physical equivalence, for the physical field $\mathbf{E}(\mathbf{r},t) = \mathrm{Re}[\tilde{\mathbf{E}}(\mathbf{r})e^{-i\omega t}]$, between a symmetry transformation and a time delay. (The simpler (3) is then just the infinitesimal version of (4).) For our polychromatic field, this equivalence at the level of physical fields still makes sense, and — for the case of coordinated rotations — it reads

$$R(\gamma\alpha)\mathbf{E}\big(R^{-1}(\alpha)\mathbf{r},t\big) = \mathbf{E}(\mathbf{r},t+\tau\alpha), \tag{5}$$

where τ is a constant with units of time, which specifies how much time delay is accrued by the field per unit rotation angle α for a coordinated rotation with coordination parameter γ.

This relationship is now a fully formed base which can be formally analysed to characterize the optical states with coordinated-rotation invariance, which we have reported previously in Ref. 1. Importantly, when this general theorem for arbitrary fields is restricted to only monochromatic waves, one recovers the previously-known results for that case.[8]

That said, although the generator eigenfunction relation (3) loses much of its value in this setting, it is still instructive to understand the symmetry group at play, as well as its generator, which corresponds to the infinitesimal version of (5). Intuitively, this should be a combination of the OAM L and SAM S (with both operators understood to be the z components of the respective vectors, within paraxial optics), weighted by the coordination parameter:

$$J_\gamma = L + \gamma S. \tag{6}$$

To understand this generator in more detail, the key starting point is the rotation symmetry group of paraxial optics: this is given by a direct product of two copies of the rotation group, $\mathrm{U}(1) \cong \mathrm{SO}(2)$, since within paraxial optics the polarization can be rotated about the optical axis independently of the spatial dependence.[20,21] This direct product, $\mathrm{U}(1)\times\mathrm{U}(1)$, forms a flat torus (as the topological product of two circles), and the subgroup of coordinated rotations forms a straight line through it, depicted in Fig. 2(f).

This subgroup, generated by J_γ, turns out to be in exact correspondence with the torus knot traced by the polarization trefoil of the beam, which we analysed in Fig. 2(e), if the torus that contains the torus knot is flattened out. This means, therefore, that the subgroup generated by J_γ has the same knotted topology as the beam itself, which motivates the name 'torus-knot angular momentum' (TKAM) for J_γ, and provides a remarkable connection between the geometric, topological and algebraic aspects of this operation.

4. THE POLARIZATION SINGULARITY

Having explored the torus-knot topology produced by these beam combinations, we now turn to an in-depth look at the nature of the optical singularity at their core. In essence, we have shown the structure created by the different orientations of the trefoils in Fig. 1(b), but this simply raises deeper questions: what happens at the center? and how does it interact with the points close to it?

At the center itself, the polarization is circular, since the 2ω field is in a LG field with zero intensity on the optical axis, leaving only the circularly-polarized fundamental there. However, if we step away from the center, we start getting a contribution from the 2ω beam, and this will tend to make the Lissajous figure of the field triangular – first slightly, and then with increasing sharpness – as shown in Fig. 3(b). Most importantly, the *orientation* of the resulting triangle will depend on the direction that we choose to displace our viewpoint away from the optical axis. As such, our beams contain a Lissajous singularity,[22–25] of a completely novel kind.

At its core, our optical singularities are singularities in the *orientation* of (the Lissajous figure of) the polarization of the beam. As such, if we want a quantitative understanding of this singularity – and, particularly, if we want a single numerical function which codifies it – then we require a numerical measure of the orientation of the bicircular Lissajous trefoil.

Within linear optics, the orientation of the polarization ellipse is obtained by looking at the 2×2 polarization matrix $\langle E_i E_j\rangle$ (the time average of the quadratic products of the electric field components), whose eigenvectors

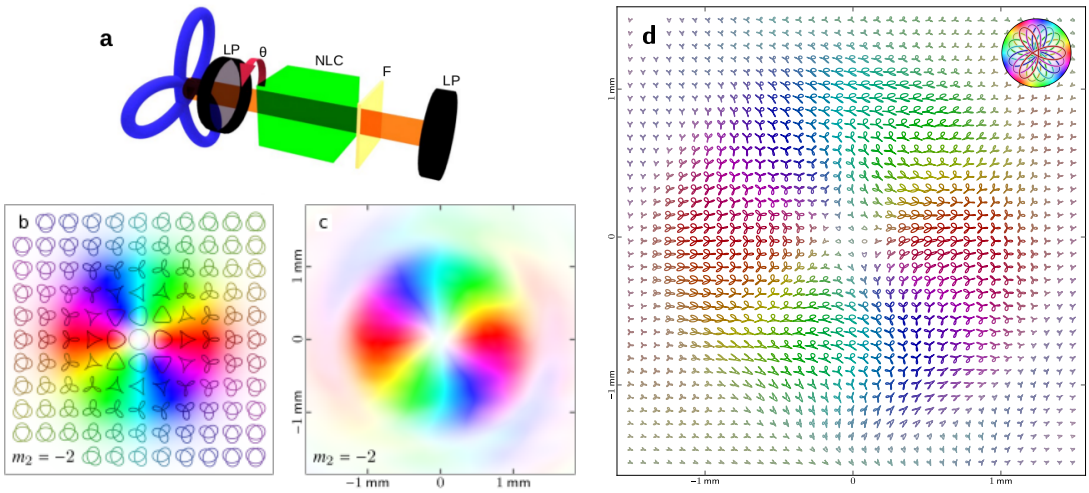

Figure 3. Polarization singularity in torus-knot beams, and its experimental probing. (a) Idealized experimental scheme for nonlinear polarization tomography: the bicircular field is passed through a linear polarizer LP, a nonlinear crystal NLC which produces a further second harmonic from the fundamental, a filter F that eliminates the fundamental, and a further linear polarizer, and then detected. The whole stack is then rotated by an angle θ over an entire revolution; the output of the method is the Fourier components of the signal over θ. (b) Lissajous field for a torus-knot beam, showing the changes to the Lissajous figure between a circle at the center and the full bicircular trefoil at mid-beam. The colour background is the $T_{3,3}$ field tensor. (c) Experimental measurement of a phase vortex in $T_{3,3}$. (d) Experimental reconstruction of the Lissajous field. Figure reproduced from Ref. 1.

point along the major and minor axis of the polarization ellipse. For bicircular combinations, however, this measure is not appropriate, since it is symmetric under rotations of the electric field by 180° but not by 120°, and the symmetry of the orientation measure needs to match the symmetry of the Lissajous figure.

However, this combination does point to an obvious direction to try: simply increasing the number of factors in the time average, from quadratic to cubic, giving the rank-3 tensor $\langle E_i E_j E_k \rangle$. This is a much bigger object than the quadratic $\langle E_i E_j \rangle$, with four linearly independent components in two dimensions, so extracting a single numerical measure of orientation requires an additional layer of analysis. This additional layer is the multipole decomposition of this tensor into its components along irreducible representations of the rotation group SO(2), which suggests the tensor measure

$$T_{3,3} = \left\langle (E_x + iE_y)^3 \right\rangle \tag{7}$$

as the combination with the correct symmetry – and, indeed, this produces precisely the desired results, with $\arg(T_{3,3})(\mod 120°)$ providing the orientation angle of the Lissajous trefoil. (This is the orientation measure shown in the background of Fig. 3(b).) More generally, this tensor is part of a wider family of measures,

$$T_{\ell,n} = \left\langle (E_x(t) + iE_y(t))^{\ell} \left(E_x(t)^2 + E_y(t)^2\right)^{\frac{n-\ell}{2}} \right\rangle, \tag{8}$$

which includes the 'other half' of the raw tensor $\langle E_i E_j E_k \rangle$, in the form of a dipole-representation component $T_{1,3} = \left\langle (E_x + iE_y)\left(E_x(t)^2 + E_y(t)^2\right)\right\rangle$ that can be used to describe 'true' vector-vortex singularities that are stable against decomposition into individual C-points.

In addition to this, our orientation measure, $T_{3,3}$, can be directly measured in a laboratory setting. This required the development of the first nonlinear polarization tomography protocol, a brief schematic of which is sketched in Fig. 3(a). (In a realistic experimental implementation, such as that in Ref. 1, a more stable but optically-equivalent configuration must be used.) As we show in Ref. 1, this nonlinear tomography protocol exactly measures $T_{3,3}$, with an example of the experimental observations shown in Fig. 3(c). Even more strongly, the measurement results can be used to provide a full reconstruction of the Lissajous figure of the field polarization at each point in the image, with the breakthrough measurements (subject to some noise and cross-talk between the modes) shown in Fig. 3(d).

5. CONSERVATION OF THE TORUS-KNOT ANGULAR MOMENTUM IN NONLINEAR OPTICAL INTERACTIONS

Having explored the structure of the torus-knot beams in detail, including their topology and their symmetry generator, it is also worth asking whether they take part in nontrivial optical interactions. This is particularly interesting in the context of high-harmonic generation, which is a demanding testbed for conservation laws in nonlinear optics.[18,26–32]

High-harmonic generation (HHG) is the flagship process of attosecond science and strong-field physics.[33] At its essence, HHG is a high-order frequency up-conversion process in which a large number of photons of an intense, long-wavelength infrared driving field gets parametrically up-converted into single photons of high-frequency XUV radiation. This process occurs at high intensity, and it is generally far from the perturbative regime, which results in a long, flat plateau of harmonics of the driving field which can span hundreds an even thousands of harmonic orders.[34] The core dynamics of the emission, at a microscopic level, are given by the 'three-step model',[35,36] in which the driving laser (1) removes an electron from one of the atoms in the target gas jet through optical tunnel ionization, after which (2) the electron propagates in the continuum driven by the laser field, and eventually (3) recombines with its parent ion, emitting its kinetic energy as a high-frequency photon.

When the infrared driving field is replaced by a high-intensity bicircular combination, this picture is largely unchanged: the field now has three maxima per period, each of which drives an ionization burst which produces electrons that eventually recollide with the parent ion and recombine, emitting an attosecond burst of radiation that is polarized along the direction of the velocity of the electron at the moment of recollision. This produces a train of attosecond pulses, each of which is linearly polarized and oriented at 120° to its neighbours.

We can then go further, and provide this bicircular driving field with a torus-knot topology by giving nonzero OAM to its two frequency components, as depicted in Fig. 4. Once we do this, the experiment becomes symmetric under coordinated rotations, with the coordination parameter γ of the drivers. As such, the optical response – i.e., the high-harmonic emission – must share this symmetry, and our previous attosecond pulse train gets transformed into a *spiral* of attosecond pulses, whose polarization twists as the spiral twists helically in divergence azimuth and time.

To see this practically, we performed simulations of the harmonic emission using the Strong-Field Approximation,[37–39] which we report in detail in Ref. 2. The results, shown in Fig. 5, agree exactly with this precision, showing a clear helical intensity distribution. The polarization along this helix, which we measure using the

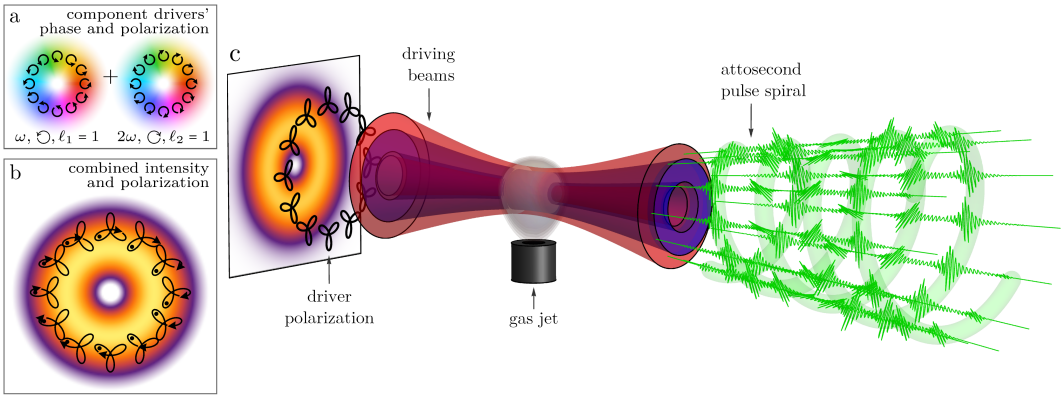

Figure 4. High-harmonic generation driven by a torus-knot beam. (a) Component ω and 2ω drivers. (b) Combined intensity and polarization of the driving beam. (c) Schematic of the configuration, with the driving beams impinging on a target gas jet. The resulting harmonic emission forms a spiral of attosecond pulses with a twisted polarization, which shares the coordinated-rotation symmetry of the driving fields. Figure reproduced from Ref. 2.

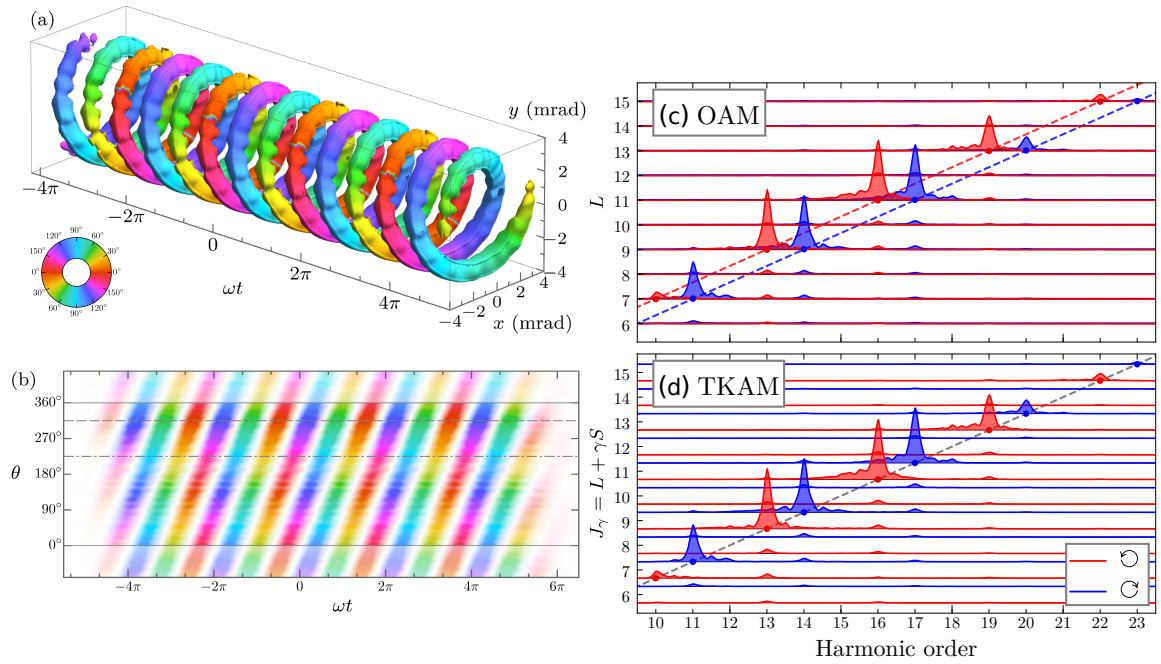

Figure 5. Simulated harmonic emission from the configuration in Fig. 4. (a) Isointensity contour of the harmonic emission in the time and angle-divergence domain, colored according to the time-specific orientation measure $T_{2,2}(\mathbf{r},t)$ (as given in the color wheel to lower left). (b) Density map of $T_{2,2}(\mathbf{r},t)$ over divergence azimuthal angle and time, showing the twisted-spiral structure of the attosecond-pulse emission. (c) Fourier transform of the results in (a,b) over time (giving harmonic order) and angle (giving OAM L), with the two counter-rotating polarizations in red and blue. (d) Displacing these plots by γS produces a single straight line, corresponding to the conservation of TKAM in the nonlinear optical interaction. Figure reproduced from Ref. 2.

time-windowed average quadrupole field moment tensor,

$$T_{2,2}(\mathbf{r},t) = \int_{-\infty}^{\infty} (E_x^{(\mathrm{xuv})}(\mathbf{r},t') + iE_y^{(\mathrm{xuv})}(\mathbf{r},t'))^2 e^{-(t'-t)^2/2\sigma^2}\,\mathrm{d}t', \tag{9}$$

with a window width of $\sigma = 15^\circ/\omega$, twists smoothly as required by the symmetry.

Moreover, we can go beyond this, and Fourier-transform this emission from the time to the frequency domain and from the angle to the angular-momentum domain. When this latter transform is done naively, producing separate OAM spectra for each of the two orthogonal circular polarizations, as shown in Fig. 5(c), the result is two separate lines, but if we take the symmetry of the drivers into account and we shift these two spectra by γ times the spin, to plot the TKAM spectrum of the beam, the two separate trends fuse into a single straight line to the origin. That is, we observe explicitly that the TKAM J_γ of the qth harmonic is q times the TKAM of the fundamental driver, which is the smoking-gun evidence of the conservation of TKAM in nonlinear optics.[2]

6. OUTLOOK

As we have seen, the torus-knot beams we have constructed prove that a new, infinite class of coordinated-rotation symmetries is possible for optical beams, once the restriction to monochromatic waves is lifted. This produces new knotted topologies and new optical singularities, which offer vast new theoretical vistas and connections but which are also cleanly accessible to experiment.

These beams have direct applications to high-harmonic generation (a setting which directly inspired the developments we report here, both via the existence of bicircular polarizations themselves[17] as well as through investigations on what happens if the two components in the bicircular superposition have different *linear* momentum[32]), where they offer a simple way to obtain bright sources of short-wavelength light with controllable

orbital angular momentum, with potential applications in magnetic and molecular spectroscopies as well as in microscopy and lithography.

More generally, the torus-knot beams raise a multitude of questions, including their relationship to quantum mechanics (can a single-photon state have a well-defined TKAM with non-half-integer γ, as discussed in Ref. 8? what about a few-photon state?) but also e.g. the possibility of replicating these structures and topologies within a spinor condensate of cold atoms.[40] Finally, and more broadly, the discovery of torus-knot optical beams is an example of the structures which were previously unseen and which become discoverable using the views and perspectives of strong-field physics – a class which also includes the discovery of beams of light with self-torque[41] –, and particularly its focus on a time-domain understanding of the field and the emphasis on polychromatic combinations as a tool for exploration. This class is likely to extend much further, so we hope that the work presented here serves as inspiration to explore that territory in other contexts, in optics and beyond.

ACKNOWLEDGMENTS

This work was performed in collaboration with G. J. Machado, V. Vicuña-Hernández, A. Picón, A. Celi, L. Rego, J. San Román, K. M. Dorney, H. C. Kapteyn, M. M. Murnane, L. Plaja, C. Hernández-García, J. P. Torres and M. Lewenstein. G.J.M., V.V.-H. and J.P.T. performed the experiment reported in Ref. 1 and reproduced in Fig. 3. L.R., L.P. and C.H.-G. performed the simulations reported in Ref. 2 and reproduced in Fig. 5. This work was funded by a Cellex-ICFO-MPQ Fellowship, the Spanish Ministry MINECO (National Plan 15 Grant: FISICATEAMO No. FIS2016-79508-P, SEVERO OCHOA No. SEV-2015-0522, FPI), European Social Fund, Fundació Cellex, Generalitat de Catalunya (AGAUR Grant No. 2017 SGR 1341 and CERCA/Program), ERC AdG NOQIA, ERC AdG OSYRIS, EU FETPRO QUIC, and the National Science Centre, Poland-Symfonia Grant No. 2016/20/W/ST4/00314.

REFERENCES

[1] Pisanty, E., Machado, G. J., Vicuña-Hernández, V., Picón, A., Celi, A., Torres, J. P., and Lewenstein, M., "Knotting fractional-order knots with the polarization state of light," *Nat. Photon.* **13**(8), 569–574 (2019).

[2] Pisanty, E., Rego, L., San Román, J., Picón, A., Dorney, K. M., Kapteyn, H. C., Murnane, M. M., Plaja, L., Lewenstein, M., and Hernández-García, C., "Conservation of torus-knot angular momentum in high-order harmonic generation," *Phys. Rev. Lett.* **122**(20), 203201 (2019).

[3] Allen, L., Beijersbergen, M. W., Spreeuw, R. J. C., and Woerdman, J. P., "Orbital angular momentum of light and the transformation of Laguerre-Gaussian laser modes," *Phys. Rev. A* **45**(11), 8185–8189 (1992).

[4] Torres, J. P. and Torner, L., eds., [*Twisted Photons: Applications of Light with Orbital Angular Momentum*], Wiley, Weinheim (2011).

[5] Andrews, D. L. and Babiker, M., eds., [*The Angular Momentum of Light*], Cambridge University Press, Cambridge (2012).

[6] Gbur, G., [*Singular optics*], CRC Press, Boca Raton (2016).

[7] Rubinsztein-Dunlop, H., Forbes, A., Berry, M. V., Dennis, M. R., Andrews, D. L., Mansuripur, M., Denz, C., Alpmann, C., Banzer, P., Bauer, T., Karimi, E., Marrucci, L., Padgett, M., Ritsch-Marte, M., Litchinitser, N. M., Bigelow, N. P., Rosales-Guzmán, C., Belmonte, A., Torres, J. P., Neely, T. W., Baker, M., Gordon, R., Stilgoe, A. B., Romero, J., White, A. G., Fickler, R., Willner, A. E., Xie, G., McMorran, B., and Weiner, A. M., "Roadmap on structured light," *J. Opt.* **19**(1), 013001 (2017).

[8] Ballantine, K. E., Donegan, J. F., and Eastham, P. R., "There are many ways to spin a photon: Half-quantization of a total optical angular momentum," *Sci. Adv.* **2**(4), e1501748 (2016).

[9] Turpin, A., Loiko, Y. V., Peinado, A., Lizana, A., Kalkandjiev, T. K., Campos, J., and Mompart, J., "Polarization tailored novel vector beams based on conical refraction," *Opt. Express* **23**(5), 5704–5715 (2015).

[10] Turpin, A., Loiko, Y. V., Kalkandjiev, T. K., and Mompart, J., "Conical refraction: fundamentals and applications," *Laser Photon. Rev.* **10**(5), 750–771 (2016).

[11] Freund, I., "Optical Möbius strips in three-dimensional ellipse fields: I. Lines of circular polarization," *Opt. Commun.* **283**(1), 1–15 (2010).

[12] Freund, I., "Optical Möbius strips in three-dimensional ellipse fields: II. Lines of circular polarization," *Opt. Commun.* **283**(1), 16–28 (2010).
[13] Bauer, T., Banzer, P., Karimi, E., Orlov, S., Rubano, A., Marrucci, L., Santamato, E., Boyd, R. W., and Leuchs, G., "Observation of optical polarization Möbius strips," *Science* **347**(6225), 964–966 (2015).
[14] Bauer, T., Neugebauer, M., Leuchs, G., and Banzer, P., "Optical polarization Möbius strips and points of purely transverse spin density," *Phys. Rev. Lett.* **117**(1), 013601 (2016).
[15] Bauer, T., Banzer, P., Bouchard, F., Orlov, S., Marrucci, L., Santamato, E., Boyd, R. W., Karimi, E., and Leuchs, G., "Multi-twist polarization ribbon topologies in highly-confined optical fields," *New J. Phys.* **21**(5), 053020 (2019).
[16] Pisanty, E., "Torus-knot light beams." Zenodo, doi:10.5281/zenodo.2597667 (2018).
[17] Fleischer, A., Kfir, O., Diskin, T., Sidorenko, P., and Cohen, O., "Spin angular momentum and tunable polarization in high-harmonic generation," *Nature Photon.* **8**(7), 543–549 (2014).
[18] Pisanty, E., Sukiasyan, S., and Ivanov, M., "Spin conservation in high-order-harmonic generation using bicircular fields," *Phys. Rev. A* **90**(4), 043829 (2014).
[19] Sugic, D., Dennis, M. R., Nori, F., and Bliokh, K. Y., "Knotted polarizations and spin in three-dimensional polychromatic waves," *Phys. Rev. Res.* **2**(4), 042045 (2020).
[20] Barnett, S. M., Allen, L., Cameron, R. P., Gilson, C. R., Padgett, M. J., Speirits, F. C., and Yao, A. M., "On the natures of the spin and orbital parts of optical angular momentum," *J. Opt.* **18**(6), 064004 (2016).
[21] Van Enk, S. and Nienhuis, G., "Spin and orbital angular momentum of photons," *Europhys. Lett.* **25**(7), 497–501 (1994).
[22] Kessler, D. A. and Freund, I., "Lissajous singularities," *Opt. Lett.* **28**(2), 111–113 (2003).
[23] Freund, I., "Bichromatic optical Lissajous fields," *Opt. Commun.* **226**(1–6), 351–376 (2003).
[24] Freund, I., "Polarization critical points in polychromatic optical fields," *Opt. Commun.* **227**(1), 61–71 (2003).
[25] Freund, I., "Polychromatic polarization singularities," *Opt. Lett.* **28**(22), 2150–2152 (2003).
[26] Perry, M. D. and Crane, J. K., "High-order harmonic emission from mixed fields," *Phys. Rev. A* **48**, R4051–R4054 (Dec 1993).
[27] Bertrand, J. B., Wörner, H. J., Bandulet, H.-C., Bisson, É., Spanner, M., Kieffer, J.-C., Villeneuve, D. M., and Corkum, P. B., "Ultrahigh-order wave mixing in noncollinear high harmonic generation," *Phys. Rev. Lett.* **106**, 023001 (Jan 2011).
[28] Zürch, M., Kern, C., Hansinger, P., Dreischuh, A., and Spielmann, C., "Strong-field physics with singular light beams," *Nature Phys.* **8**(10), 743–746 (2012).
[29] Gariepy, G., Leach, J., Kim, K. T., Hammond, T. J., Frumker, E., Boyd, R. W., and Corkum, P. B., "Creating high-harmonic beams with controlled orbital angular momentum," *Phys. Rev. Lett.* **113**(15), 153901 (2014).
[30] Kong, F., Zhang, C., Bouchard, F., Li, Z., Brown, G. G., Ko, D. H., Hammond, T., Arissian, L., Boyd, R. W., Karimi, E., et al., "Controlling the orbital angular momentum of high harmonic vortices," *Nature Commun.* **8**, 14970 (2017).
[31] Gauthier, D., Ribič, P. R., Adhikary, G., Camper, A., Chappuis, C., Cucini, R., DiMauro, L., Dovillaire, G., Frassetto, F., Géneaux, R., et al., "Tunable orbital angular momentum in high-harmonic generation," *Nature Commun.* **8**, 14971 (2017).
[32] Hickstein, D. D., Dollar, F. J., Grychtol, P., Ellis, J. L., Knut, R., Hernández-García, C., Zusin, D., Gentry, C., Shaw, J. M., Tingting Fan, K. M. D., Becker, A., Jaroń-Becker, A., Kapteyn, H. C., Murnane, M. M., and Durfee, C. G., "Non-collinear generation of angularly isolated circularly polarized high harmonics," *Nature Photon.* **9**(11), 743 – 750 (2015).
[33] Krausz, F. and Ivanov, M., "Attosecond physics," *Rev. Mod. Phys.* **81**(1), 163–234 (2009).
[34] Popmintchev, T., Chen, M.-C., Popmintchev, D., Arpin, P., Brown, S., Ališauskas, S., Andriukaitis, G., Balčiunas, T., Mücke, O. D., Pugzlys, A., Baltuška, A., Shim, B., Schrauth, S. E., Gaeta, A., Hernández-García, C., Plaja, L., Becker, A., Jaron-Becker, A., Murnane, M. M., and Kapteyn, H. C., "Bright coherent ultrahigh harmonics in the keV X-ray regime from mid-infrared femtosecond lasers," *Science* **336**(6086), 1287–1291 (2012).

[35] Corkum, P. B., "Plasma perspective on strong field multiphoton ionization," *Phys. Rev. Lett.* **71**(13), 1994–1997 (1993).

[36] Kulander, K. C., Schafer, K. J., and Krause, J. L., "Dynamics of short-pulse excitation, ionization and harmonic conversion," in [*Super-Intense Laser Atom Physics*], Piraux, B., L'Huillier, A., and Rzążewski, K., eds., *NATO Advanced Studies Institute Series B: Physics* **316**, 95–110, Plenum, New York (1993).

[37] Lewenstein, M., Balcou, P., Ivanov, M. Y., A. L'Huillier, and Corkum, P. B., "Theory of high-harmonic generation by low-frequency laser fields," *Phys. Rev. A* **49**, 2117–2132 (Mar 1994).

[38] Pérez-Hernández, J. A., Roso, L., and Plaja, L., "Harmonic generation beyond the Strong-Field Approximation: the physics behind the short-wave-infrared scaling laws," *Opt. Express* **17**(12), 9891–9903 (2009).

[39] Hernández-García, C., Román, J. S., Plaja, L., and Picón, A., "Quantum-path signatures in attosecond helical beams driven by optical vortices," *New J. Phys.* **17**(9), 093029 (2015).

[40] Jayaseelan, M., *Topological atom-optics with spinor Bose–Einstein condensates*, PhD thesis, University of Rochester (2021). handle:1802/36398, chapter 5.

[41] Rego, L., Dorney, K. M., Brooks, N. J., Nguyen, Q. L., Liao, C.-T., San Román, J., Couch, D. E., Liu, A., Pisanty, E., Lewenstein, M., Plaja, L., Kapteyn, H. C., Murnane, M. M., and Hernández-García, C., "Generation of extreme-ultraviolet beams with time-varying orbital angular momentum," *Science* **364**(6447), eaaw9486 (2019).